 doi:10.20944/preprints202102.0065.v1

Article

Research on high-pressure hydrochloric acid leaching of scandium, aluminum and other valuable components from the non-magnetic residues obtained from red mud after iron removal

Dmitry Zinoveev [1,*], Pavel Grudinsky [1], Ekaterina Zhiltsova [1,2], Darya Grigoreva [1], Anton Volkov [3], Valery Dyubanov [1] and Alexander Petelin [4]

[1] Laboratory of Physical Chemistry and Technology of Iron Ore Processing, A.A. Baikov Institute of Metallurgy and Materials Science, Russian Academy of Science, 49 Leninsky prosp, Moscow 119334, Russia; dzinoveev@imet.ac.ru (D.Z.), pgrudinskiy@imet.ac.ru (P.G.), dashagrgrv121@gmail.com (D.G.), vdyubanov@imet.ac.ru (V.D.)

[2] D. Mendeleev University of Chemical Technology of Russia, 9 Miusskaya square, Moscow 125047, Russia; ekaterinazhiltsova@yandex.ru (E.Z.)

[3] I. P. Bardin Central Research Institute of Ferrous Metallurgy, 23/9 bdg. 2, Radio str., Moscow 105005, Russia; rhenium@list.ru (A.V.)

[4] Department of Energy-Efficient and Resource-Saving Industrial Technologies, National University of Science & Technology (MISIS), 4 Leninsky prosp., Moscow 119049, Russia; sasha@misis.ru (A.P.)

* Correspondence: dzinoveev@imet.ac.ru; Tel.: +7-499-135-94-49

Abstract: Red mud is a hazardous waste of alumina industry that contains high amounts of iron, aluminum, titanium and REEs. One of the promising methods for the extraction of iron from red mud is carbothermic reduction with the addition of sodium salts. This research focuses on the process of hydrochloric high-pressure acid leaching using 10–20% HCl of two samples of non-magnetic tailings obtained by 60-minute carbothermic roasting of red mud at 1300 °C and the mixture of 84.6 wt. % of red mud and 15.4 wt. % Na_2SO_4 at 1150 °C, respectively, with subsequent magnetic separation of metallic iron. An influence of temperature, leaching duration, solid-to-liquid-ratio and acid concentration on dissolution behavior of Al, Ti, Mg, Ca, Si, Fe, Na, La, Ce, Pr, Nd, Sc, Zr were studied. Based on the investigation of the obtained residues, mechanism of passing of valuable elements into the solution was proposed. It has shown that 90% Al, 91% Sc and above 80% of other REEs can be dissolved under optimal conditions; Ti can be extracted into the solution or the residue depending on the leaching temperature and acid concentration. Based on the research results, novel flowsheets for red mud treatment were developed.

Keywords: red mud; bauxite residue; reduction roasting; sodium sulfate; magnetic separation; alumina; high pressure acid leaching; hydrochloric acid; recycling; utilization

1. Introduction

Red mud is a solid waste generated during the extraction of alumina from bauxite ores by the Bayer method [1]. At present time, the main treatment methods for red mud include stockpiling by damming, direct sea-fill, and sea-fill after neutralization [2]. Globally, about 4 billion tons of red mud are currently stored [3,4]. The lack of efficient processing technologies is the main reason why red mud is out of use and accumulated in special sludge storage facilities, which have an adverse impact on the environment and even have led to the technogenic catastrophe [3]. It has found that red mud is proved to be a promising material for the obtaining of coagulants and can be used as an adsorbent for heavy metals in wastewater; it can also be utilized in a wide range of catalytic applications [5], as well as for a production of various building materials [6].

The typical contents of valuable components in red mud such as Ti, Si, Fe, Na and Al are 2–12%, 1–9%, 14–45%, 1–6% and 5–14%, respectively [7]. Moreover, red mud also

Preprints (www.preprints.org) | NOT PEER-REVIEWED | Posted: 1 February 2021 doi:10.20944/preprints202102.0065.v1

contains a small proportion of rare-earth metals (REEs) in the range of 0.05–0.17% [8]. It is important to note that Sc content in red mud is in the range of 0.013–0.039% [9] that is quite significant. The actual composition of red mud depends on the bauxite mineralogy and different technological parameters of the Bayer process [10]. Iron content in red mud is comparable with poor iron ore [11] that is an important driver for research on the processing of red mud.

Many processes were proposed for recovery of valuable components from red mud [8,12,13]. In last years, there is a high interest for selective recovery of scandium [9,14,15]. Direct leaching processes using different lixiviants such as alkaline solutions [16,17], hydrochloric and sulfuric acids [18–24], organic acids [25,26] and ionic liquids [27,28] were thoroughly investigated. However, the direct leaching methods are either non-selective or ineffective for the extraction of titanium and REEs.

High content of iron in red mud is the main hindering factor for the extraction of REEs from the solutions obtained by red mud acid leaching [28,29]. For this reason, the most promising way for comprehensive recycling of red mud is combined pyro- and hydrometallurgical methods with a recovery of iron by pyrometallurgical methods followed by leaching of valuable components from the iron-depleted red mud [30]. The main pyrometallurgical ways for iron recovery from red mud are reduction smelting and carbothermic roasting with subsequent magnetic separation of reduced iron. The reduction smelting either requires high temperature and uses different fluxes such as CaO [31], SiO_2 [32], CaO–SiO_2 mixtures [29], Al_2O_3 [33], or needs for preliminary extraction of alumina [34] for the obtaining of slags with low viscosity and melting temperature. The more favorable way is the carbothermic roasting – magnetic separation approach due to a lower energy consumption compared with a reduction smelting. Many studies [35–40] have shown that direct carbothermic roasting of red mud with different additions followed by magnetic separation results in the obtaining of iron concentrates with about 95% of iron content at the temperatures below 1200 °C.

There are several studies describing leaching of valuable elements from tailings obtained by carbothermic roasting of red mud with alkaline salts followed by magnetic separation. Such two-step process followed by alumina extraction using alkaline leaching was proposed for red mud treatment [41,42], but alkaline leaching of the tailings led to the recovery only alumina and sodium without the extraction of other valuable elements. It has shown [43] that the addition of sodium salts such as Na_2CO_3 and Na_2SO_4 significantly improves the recovery of Al, Fe, Ti and Si from the tailings by sulfuric acid leaching at 30 °C.

The dissolution of silicon from red mud during an acid leaching can lead to formation of silica gel, which causes significant difficulties for filtration of the leached solution [44], so different methods were proposed to avoid it. The comparative atmosphere leaching of the tailings by different inorganic acids, namely, hydrochloric, nitric, sulfuric, and phosphoric [45] has indicated that only phosphoric acid allows to achieve selective removal of SiO_2 with substantial enrichment of Sc_2O_3 and TiO_2 in the residue. Suggested two-step process includes SiO_2 extraction by phosphoric acid leaching followed by Al_2O_3 extraction from the residue by the leaching using sodium hydroxide. The other approaches, which allows to avoid silica gel formation, are high-pressure acid leaching (HPAL) or using a high liquid-to-solid ratio [46]. The comparative study of the dissolution efficiency of the slags after red mud reduction smelting at atmosphere leaching and high-pressure leaching using HCl and H_2SO_4 have shown that high-pressure hydrochloric acid leaching allows to extract more than 90% Al and above 95% Y, La, and Nd, as well as up to 80% Sc with the co-dissolution of Si and Ti below 5% [29]. The use of hydrochloric acid for HPAL for the aluminum extraction in different high-silica materials, e.g. coal ash [47], resulted in higher aluminum extraction compared with other mineral acids [48].

Thus, a promising way for the extraction of valuable components from red mud is the reduction roasting with obtaining of magnetic iron concentrate and non-magnetic

Preprints (www.preprints.org) | NOT PEER-REVIEWED | Posted: 1 February 2021 doi:10.20944/preprints202102.0065.v1

tailings enriched in aluminum, titanium and REEs followed by the treatment of the tailings by high-pressure hydrochloric acid leaching.

In this paper, we study hydrochloric acid leaching of two different kinds of the tailings after carbothermic roasting and magnetic separation of red mud. The leaching behavior of major elements (Al, Ti, Ca, Si, Fe, Na, Mg) and minor elements (Sc, Y, La, Ce, Nd, Pr, Zr) under atmosphere and high-pressure conditions were investigated. The most influencing factors on the leaching process were identified, and optimal leaching conditions were determined. The obtained solutions and the solid residues were characterized by different methods, so leaching mechanism of valuable components was proposed. Two flowsheets for the processing of the both non-magnetic tailings were developed.

2. Materials and Methods

2.1. Raw Materials

Two samples of non-magnetic tailings were derived by reduction roasting – magnetic separation process of red mud (RM) from Bogoslovsky Aluminium Plant (Russian Federation, Krasnoturyinsk, 59.84°N, 60.19°E) at optimal conditions according with our previous work [49]. The first sample codenamed as without addition tailings (WAT) was obtained by reduction roasting of RM at 1300 °C during 1 hour. The second sample codenamed as sodium sulfate addition tailings (SSAT) was obtained by reduction roasting of the mixture of 84.6 wt. % RM and 15.4 wt. % Na_2SO_4 at 1150 °C during 3 hours. Both the roasted samples were ground, screened through a 300-mesh sieve, and magnetically separated using a wet method by the Davis tube XCGS–50 (Shaoxing Weibang Mining Machinery Manufacturing Co., Ltd., Zhejiang, China) at magnetic field intensity of 0.1 T. Table 1 demonstrates the chemical compositions and total iron content (TFe) of the RM, WAT, and SSAT samples.

Table 1. Chemical composition of the samples (wt. %).

Component	RM	WAT	SSAT
TFe	34.84	2.6	4.5
SiO_2	8.71	21.56	17.91
Al_2O_3	12.77	31.46	24.75
TiO_2	4.67	10.28	9.17
CaO	9.26	25.5	14.78
MgO	0.65	2.64	1.79
MnO	0.26	0.38	0.29
Na_2O	3.3	2.99	8.92
P_2O_5	0.85	0.17	0.10
S	0.48	0.44	4.77
ZrO_2	0.034	0.0846	0.0657
Sc_2O_3	0.014	0.052	0.04
Y_2O_3	0.058	0.14	0.121
Nd_2O_3	0.032	0.0887	0.0688
Pr_2O_3	0.007	0.0173	0.0149
CeO_2	0.048	0.0804	0.1218
La_2O_3	0.034	0.0786	0.0809

As can be seen, the contents of Al_2O_3, TiO_2, and REEs are significantly increased, but TFe content was considerably decreased in the WAT and SSAT samples compared with the RM sample. The compositions of both the tailings are quite similar, but they are different in sulfur and sodium contents due to the addition of Na_2SO_4 for the SSAT sample in the roasting process.

Preprints (www.preprints.org) | NOT PEER-REVIEWED | Posted: 1 February 2021 doi:10.20944/preprints202102.0065.v1

Figure 1 shows diffractograms of the WAT and SSAT samples with phase signs. The mineral compositions of the samples are quite different.

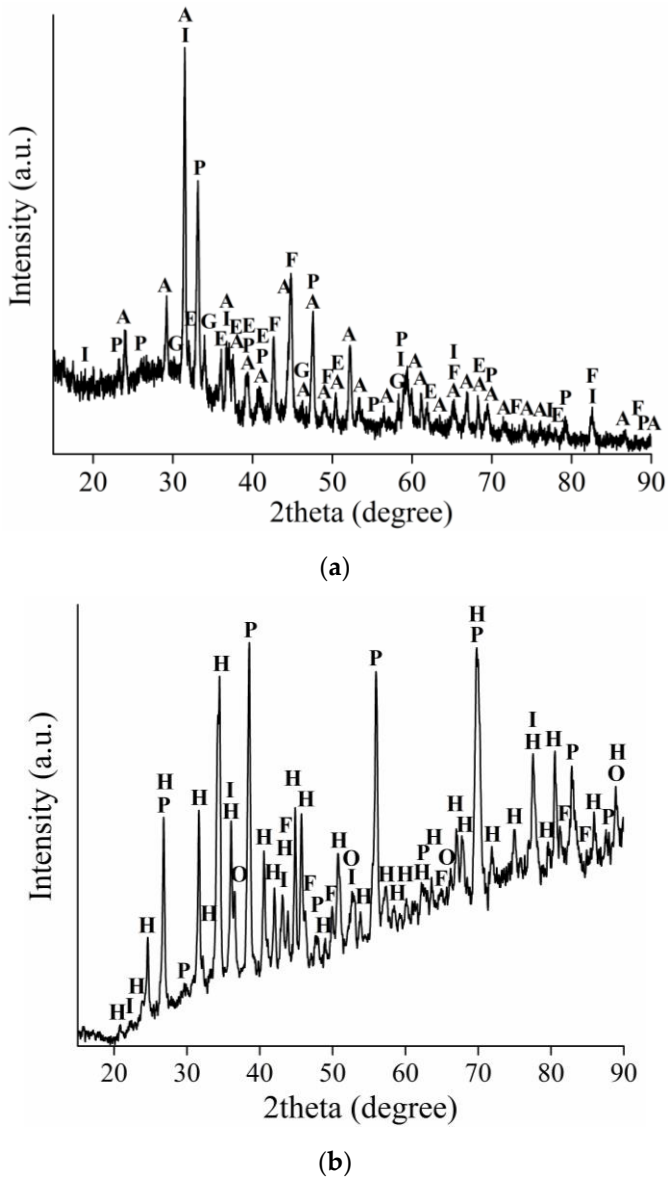

Figure 1. The XRD pattern of the WAT sample obtained using Cu-K_α radiation (**a**) and the SSAT sample obtained using Co-K_α radiation (**b**), where A – $Ca_2Al_2SiO_7$; P – $CaTiO_3$; F – Fe; G – $Ca_3Al_2Si_3O_{12}$; E – $Mg_3Al_2Si_3O_{12}$; I – $MgAl_2O_4$; H – $NaAlSiO_4$; O – CaS.

The major phases of the WAT sample are $Ca_2Al_2SiO_7$ (gehlenite), $CaTiO_3$ (perovskite), $Ca_3Al_2Si_3O_{12}$ (grossular). Also, it contains small amounts of $Mg_3Al_2Si_3O_{12}$ (pyrope), $MgAl_2O_4$ (magnesium aluminum oxide), and Fe (iron). The major phases of the SSAT sample are $NaAlSiO_4$ (nepheline) and CaS (oldhamite), which were formed by chemical reactions between Na_2SO_4 and calcium-aluminum-silicon oxides during the carbothermic roasting of red mud [49]. It should be noted an absence of gehlenite and grossular in the SSAT compared to the WAT, as well as a similarity of other minerals to the WAT sample.

2.2. Experimental Procedure

The chemical composition of the tailings and solid residues after the leaching were analyzed after an appropriate digestion using an inductively coupled plasma atomic emission spectrometer (ICP AES) Vista Pro (Varian Optical Spectroscopy Instr., Mulgrave, Australia). Additionally, the tailings and the solid residues were analyzed by

Preprints (www.preprints.org) | NOT PEER-REVIEWED | Posted: 1 February 2021 doi:10.20944/preprints202102.0065.v1

X-ray fluorescence spectrometer (XRF) ARL QUANT'X (Thermo Fisher Scientific, Ekublens, Switzerland) and AXIOSmax Advanced (PANalytical, Almelo, the Netherlands), respectively. The mother liquors and washings were analyzed by an inductively coupled plasma atomic emission spectrometer (ICP-MS) Perkin-Elmer Sciex ELAN 6100 DRC (PerkinElmer Inc., Waltham, MA, USA) and ICP AES Optima 3300RL (PerkinElmer Inc., Waltham, MA, USA). X-ray diffraction patterns (XRD) were obtained by diffractometers Difrey (JSC Scientific Instruments, Saint-Petersburg, Russian Federation) using Co-K_α radiation or ARL X'tra diffractometer (Thermo Fisher Scientific, Ekublens, Switzerland) using Cu-K_α radiation with their subsequent processing by the Match! software (Crystal Impact, Bonn, Germany) [50].

The tailings was preliminary dried at 110 °C for 2 hours and then was leached using a laboratory autoclave P2004 (Shanghai Jieang Instrument Co., Shanghai, China) in 25 ml stainless steel pots with teflon inserts at a temperature in the range of 50–210 °C at stirring speed of 350 rpm and duration time of 30–90 min. Hydrochloric acid with a concentration in the range of 10–20% was used for the leaching; used solid-to-liquid ratios (S:L) were 1:5.5, 1:11, 1:16.5. As a result of the leaching, a mother liquor was obtained by vacuum filtration. The solid residue obtained by the filtration was washed with distilled water and dried at 110 °C in an air furnace for 2 hours.

The recovery degree of major and minor elements was calculated using following equations, respectively:

$$\varepsilon = 100 - (m_r \times \%MjE_r) / (m_0 \times \%MjE_0) \times 100\%, \quad (1)$$

$$\varepsilon = (\alpha \times V_{liq} + \beta \times V_{water}) / (m_0 \times \%MnE_0) \times 100\%, \quad (2)$$

where ε – element recovery degree, %; m_r – mass of the solid residue, g; m_0 – mass of the tailings, g; $\%MjE_0$ and $\%MjE_r$ – content of a major element in tailings and in the solid residue, respectively, %; $\%MnE_0$ – content of a minor element in the tailings, %; α – content of an element in mother liquor, g/l; V_{liq} – volume of mother liquor, l; β – content of an element in washing distilled water, g/l; V_{water} – volume of washing distilled water, l.

The samples before and after leaching were placed onto the carbon tape and analyzed using scanning electron microscope (SEM) VEGA 3SB (Tescan, Brno, Czech Republic) equipped by energy-dispersive X-ray analyzer (EDX) INCA SDD X-MAX (Oxford Instruments, Abingdon, UK).

3. Results

3.1. HPAL experiments with the variation of leaching temperature and HCl concentration

3.1.1. HPAL for the WAT sample

Figure 2 demonstrates the influence of leaching temperature on the recovery degree of major elements for the WAT sample. A significant simultaneous dissolution of aluminum, iron, calcium, magnesium and sodium for both the acid concentration of 10% and 20% were discovered. An increase of temperature from 70 to 170 °C led to a growth of the aluminum extraction degree from 74% to 91% for 10% HCl, while a temperature rises from 50 to 210 °C with the application of 20% HCl resulted in an increase of the aluminum recovery degree from 81% to 98%.

Silicon dissolution degree was 41% at 50 °C for diluted acid, and it decreased to less than 2% with an increase of leaching temperature above 100 °C; an increase of acid concentration also led to similarly low dissolution of silicon. These results can be explained by significant retardation of silica hydration with a HPAL temperature rise due to water released as vapor, so a partially hydrated metal reacts with hydrochloric acid to silica form. Therefore, the use of HPAL allows to avoid silica gel formation. The process can be described by the following equation [29,51]:

Preprints (www.preprints.org) | NOT PEER-REVIEWED | Posted: 1 February 2021 doi:10.20944/preprints202102.0065.v1

$$M_2SiO_{4(s)} + 4HCl_{(l)} + (4n-2)H_2O_{(l)} = 2MCl_2\ nH_2O_{(l)} + SiO_{2(filterable)}, \quad (3)$$

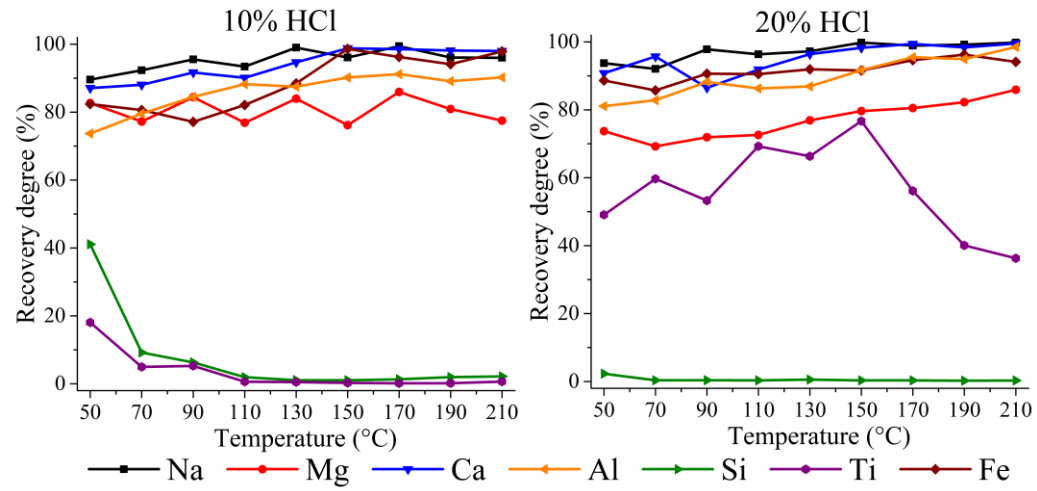

Figure 2. The effect of the temperature on recovery degree of the major elements for the leaching of the WAT sample using 10% and 20% HCl at S:L ratio = 1:11 for 60 min.

The leaching behavior of titanium is quite different for 10% and 20% acid concentration. The recovery degree of titanium for diluted acid is 18% at 50 °C; it decreases to less than 1% at temperatures above 100 °C. In contrast, the dissolution degree of titanium at 50 °C is 49% for concentrated acid; it increases to 77% with HPAL temperature rising up to 150 °C, then decreases to 36%. These results agree well with previously reported data [51,52], where perovskite is proved to be highly soluble in concentrated hydrochloric acid and poorly soluble in diluted acid. Hence, the use of high-pressure diluted hydrochloric acid leaching allows to separate selectively titanium and silicon from the other elements.

Figure 3 shows the influence of leaching temperature on the extraction degree of minor elements.

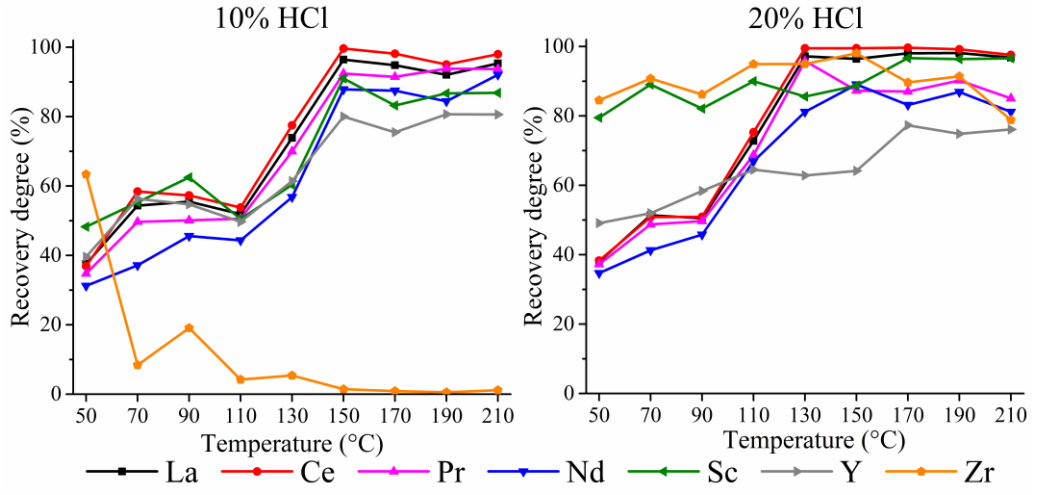

Figure 3. The effect of the temperature on recovery degree of the minor elements for the leaching of the WAT sample using 10% and 20% HCl at S:L ratio = 1:11 for 60 min.

As can be seen, for both 10% and 20% HCl the dissolution degrees of La, Ce, Pr, Nd are very similar, but the dissolution behavior of Sc and Y is rather different that is in agreement with the results of other researchers [53]. The recovery degrees of all REEs were near 40% for both the acid concentrations at 50 °C; they increase significantly with

Preprints (www.preprints.org) | NOT PEER-REVIEWED | Posted: 1 February 2021 doi:10.20944/preprints202102.0065.v1

temperature rising. REE extraction degrees have a peak with the values of more than 75% for 10% HCl at the temperatures above 150 °C. These results are also in accordance with [53], where a significant influence of the temperature on leaching of REEs from iron-removed red mud was noted. There are few differences of REE leaching using the diluted and concentrated acids. REE extraction degree for 10% HCl starts to increase dramatically at the temperature over 110 °C, and for 20% HCl such abrupt jump occurs above 90 °C. The dissolution degree of Sc is near 80–90% at the low temperatures for the concentrated acid unlike 50-60% for the diluted acid. However, a rise of the temperature up to 150 °C and above using the diluted acid led to an achievement of a plateau at a level of 83–91%, while using of the concentrated acid enabled to achieve the best extraction degrees of 96–97% in the range of 170-210 °C.

A zirconium behavior is considerably different compared with the other minor elements. The application of 10% HCl at the temperature range of 110–210 °C resulted in the recovery degrees of Zr below 5%, while the application of 20% HCl at the same range led to 78–95% Zr extraction. Therefore, either dissolution or retention in the residue can be considered for Zr recovery in the case of its economic feasibility. It should be noted that the behavior of Zr correlates with Ti qualitatively but differs quantitatively that is probably because of similarity of their properties due to the presence in the same subgroup of the periodic table.

3.1.2. HPAL for the SSAT sample

The leaching of the SSAT sample was performed starting with 90 °C to avoid a substantial silicon dissolution at temperatures below. Figure 4 depicts the effect of the temperature and the acid concentration on the extraction degree of the major elements for the SSAT sample.

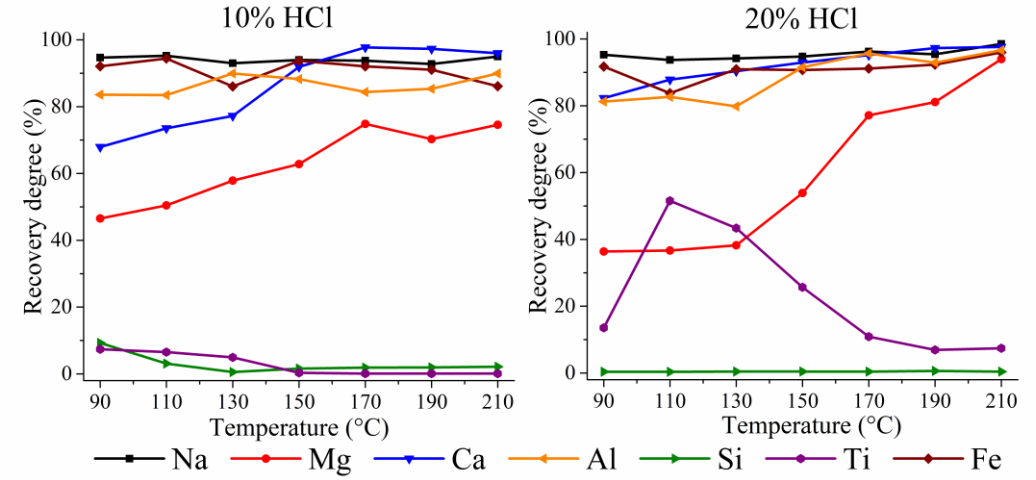

Figure 4. The effect of the temperature on the recovery degree of the major elements for the leaching of the SSAT sample using 10% and 20% HCl at S:L ratio = 1:11 for 60 min.

The curves of Fe, Al, Na, Ti, and Si are fairly similar to the ones obtained by the processing of the WAT sample, but a behavior of Mg and Ca is significantly different. As can be seen, the extraction degree of calcium for 10% acid concentration is 68% at 90 °C, whereas for the WAT sample under similar conditions it is more than 91% (Figure 2). The dissolution degree of calcium grows up with a temperature increasing and becomes above 91% only at 150 °C for both 10% and 20% acid concentration. The magnesium recovery degree rises from 46% to 74% for the diluted acid and from 36% to 94% for the concentrated acid at the range of 90–170°C. The maximum recovery degree of magnesium for the SSAT sample is 94% at 210 °C and 20% HCl concentration.

Figure 5 shows the effect of the temperature on the extraction degree of minor elements for the SSAT sample.

Preprints (www.preprints.org) | NOT PEER-REVIEWED | Posted: 1 February 2021 doi:10.20944/preprints202102.0065.v1

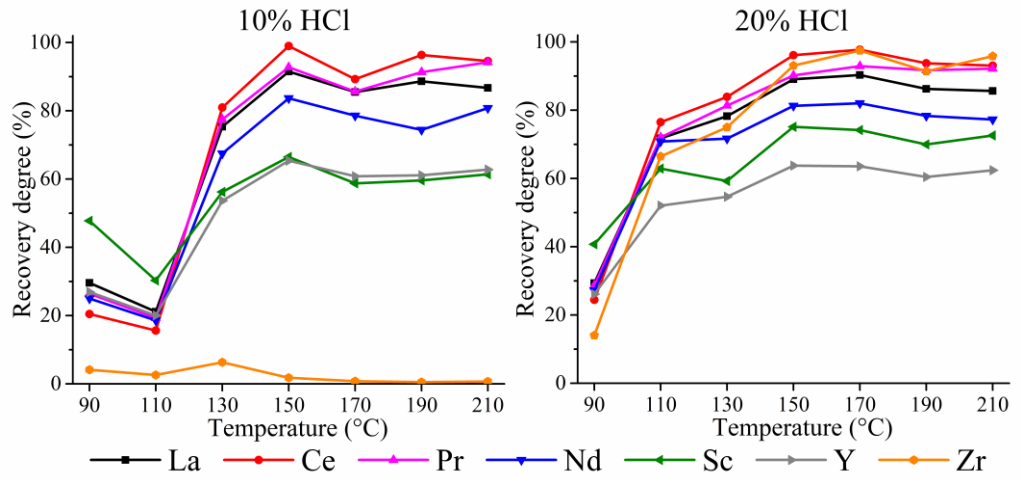

Figure 5. The effect of the temperature on the recovery degree of the minor elements for the SSAT sample using 10% and 20% HCl at S:L ratio = 1:11 for 60 min.

As can be inferred from the plots, the main factor influencing on the REE dissolution is temperature for both the WAT and SSAT sample. An increase of acid concentration also leads to a rise of the REE recovery degree at low temperatures. The extraction degrees of La, Ce, Pr, and Nd are similar in the SSAT compared to the WAT sample, but the dissolution degrees of Sc and Y are lower. The maximum recovery degrees of Sc for the WAT sample were 91% for the diluted acid and 96% for concentrated acid, wherein they were only 66% and 75% for the SSAT sample, respectively. Other REEs have also a rather lower dissolution degree for the SSAT sample. A discrepancy in dissolution behavior of elements for the WAT and SSAT samples is likely due to a difference in chemical and phase compositions; we consider it below.

3.2. The analysis of the solid residues

3.2.1. The solid residues obtained from the WAT sample

To determine the leaching mechanism, the XRD and SEM-EDX analyses of the solid residues after the leaching were performed.

Figure 6 demonstrates the elemental distribution of one of the residues obtained by HPAL of the WAT sample. It is clearly presented that the residue is a mixture of amorphous SiO_2 and minerals containing aluminum, calcium and titanium.

Figure 7 presents the XRD patterns of the WAT residues obtained at various leaching temperatures using different HCl concentrations. The WAT sample contains four aluminum phases, namely, $Ca_2Al_2SiO_7$, $Ca_3Al_2Si_3O_{12}$, $Mg_3Al_2Si_3O_{12}$, and $MgAl_2O_4$ (Figure 1), but the solid residues obtained by HPAL of the WAT sample using 10 and 20% HCl contains no gehlenite, which fully dissolves at low leaching temperatures. These results correlate with the data of other researchers [54], where gehlenite passed into the solution in 1M HCl after 3-stage leaching during 2 hours at room temperature. Aluminum in the solid residues is in $Ca_3Al_2Si_3O_{12}$, $Mg_3Al_2Si_3O_{12}$, and $MgAl_2O_4$ phases that were incompletely dissolved at the experimental conditions. It has shown [55] that grossular has a low solubility in the diluted hydrochloric acid; to decompose it fully, a high acid concentration and temperature over 130 °C are required (Figure 7). The magnesium aluminum oxide is also undissolved even at 190 °C and 20% acid concentration. $MgAl_2O_4$ is a hardly soluble phase that remains in the residue after sequential long-time treatment by 36–38% HCl и 40% HF [56]. Even high-pressure leaching by a strong HCl solution at 210°C led to substantial but still incomplete dissolution of $MgAl_2O_4$ [57]. Therefore, full aluminum extraction requires a high temperature, a strong acid concentration and using of HPAL.

Preprints (www.preprints.org) | NOT PEER-REVIEWED | Posted: 1 February 2021 doi:10.20944/preprints202102.0065.v1

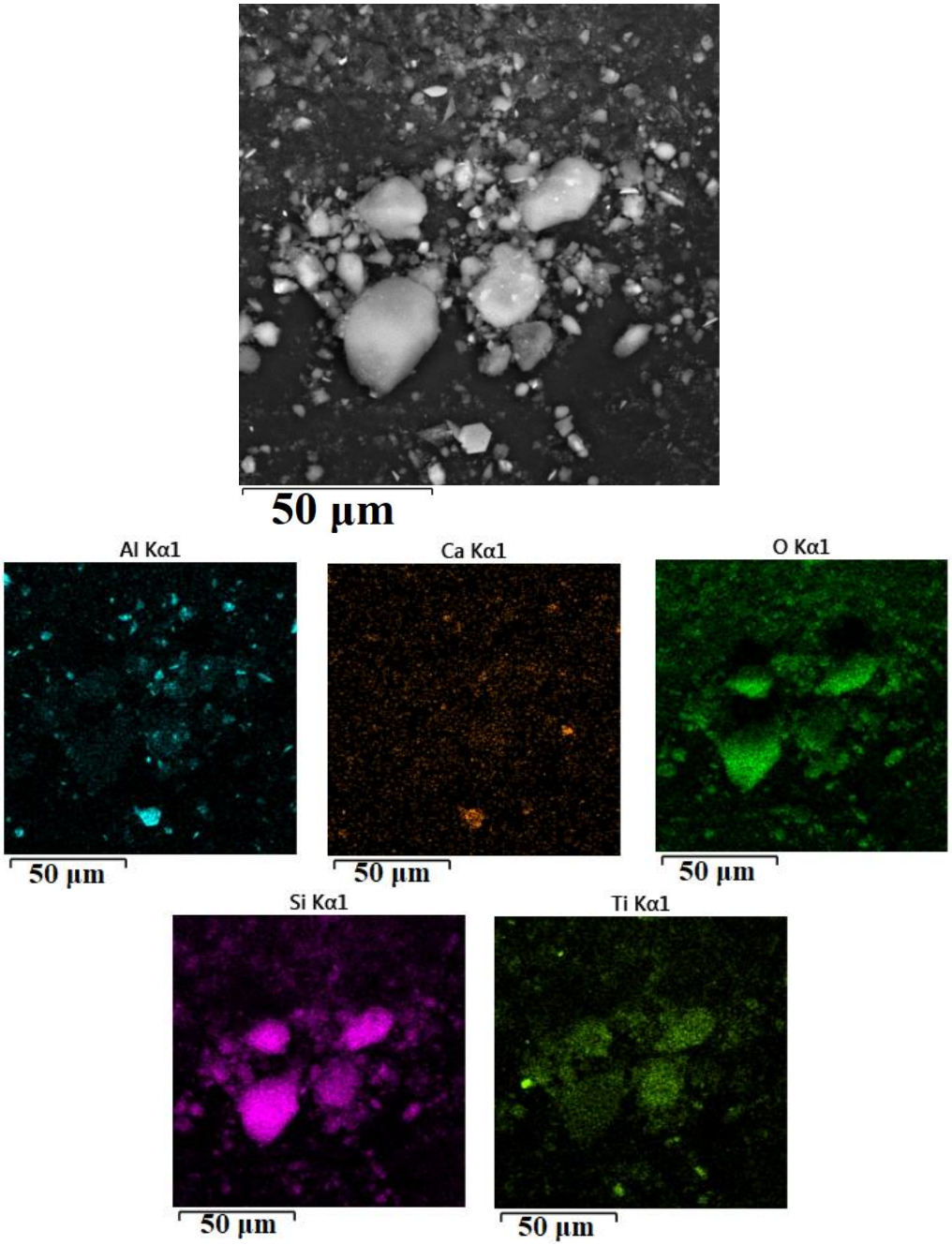

Figure 6. SEM images with the distribution of elements in the solid residue obtained by the leaching of the WAT sample using 10% HCl at 150 °C and S:L = 1:11 for 60 min.

A dissolution behavior of titanium is very different for the diluted and the concentrated acids. Figure 7a shows that perovskite exists in the solid residues after the treatment of the WAT sample by HPAL with 10% HCl up to 130 °C, and it was undetected in the residue at 190 °C.

As follows from Figure 7b, the use of 20% HCl led to full dissolution of perovskite at temperatures lower than the use of 10% HCl, but the precipitation of titanium was incomplete. The titanium extraction degree increases with leaching temperature rising (Figure 2). A similar titanium behavior in hydrochloric acid solution also was reported earlier [29,57] that is likely owing to titanium hydrolysis process [57]. The processes of dissolution and precipitation of titanium can be described as follows:

$$2CaO{\cdot}TiO_{2(s)} + 8HCl_{(l)} = 2CaCl_{2(l)} + TiCl_{4(l)} + TiO_{2(s)}\downarrow + 4H_2O_{(l)}, \quad (4)$$

$$CaO{\cdot}TiO_{2(s)} + 4HCl_{(l)} = TiOCl_{2(l)} + CaCl_{2(l)} + 2H_2O_{(l)}, \quad (5)$$

Preprints (www.preprints.org) | NOT PEER-REVIEWED | Posted: 1 February 2021 doi:10.20944/preprints202102.0065.v1

$$TiOCl_{2(l)} + (x+1)\ H_2O_{(l)} = 2HCl_{(l)} + TiO_2{\cdot}xH_2O_{(s)}\downarrow. \quad (6)$$

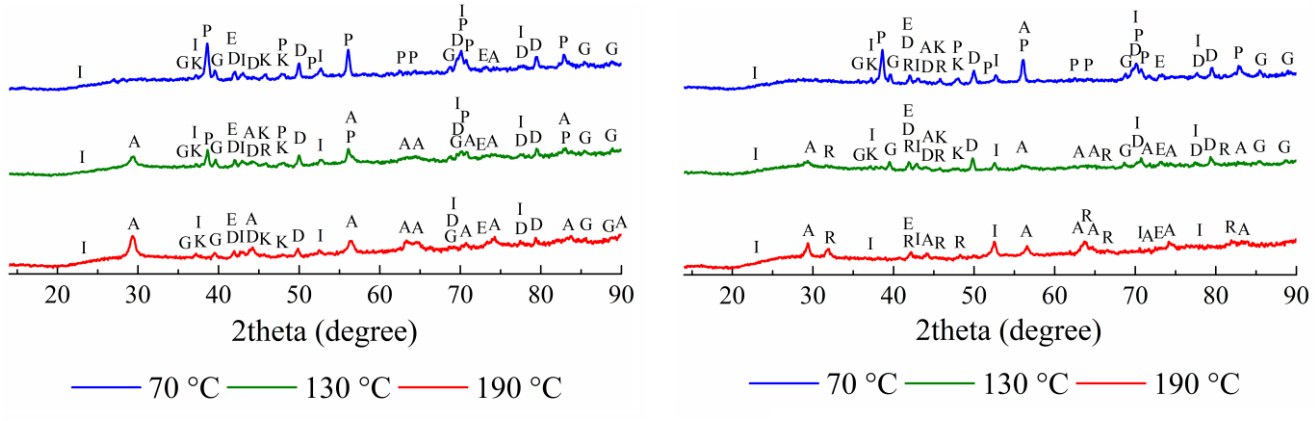

Figure 7. The XRD patterns of the solid residues after leaching of WAT sample using 10% (**a**) and 20% HCl (**b**), where P – $CaTiO_3$; A – TiO_2 (anatase); R – TiO_2 (rutile); G – $Ca_3Al_2Si_3O_{12}$; K – $Ca_3Al_2Si_3(OH)_{12}$; E – $Mg_3Al_2Si_3O_{12}$; D – $5Al_2O_3{\cdot}H_2O$; I – $MgAl_2O_4$.

Although the main part of aluminum passed into solution during HPAL, small peaks of aluminum-containing phase, $5Al_2O_3{\cdot}H_2O$, was still detected in the residues obtained at 70–190 °C using 10% HCl and at 70–130 °C using 20% HCl. Figure 8 and Table 2 also confirm the presence of this phase using SEM-EDX analyses. As reported by [58], $5Al_2O_3{\cdot}H_2O$ may be formed only under hydrothermal conditions. It is an open question how this phase has been generated during the experiments, but its formation is an unambiguously adverse factor due to a decreasing of the aluminum dissolution degree.

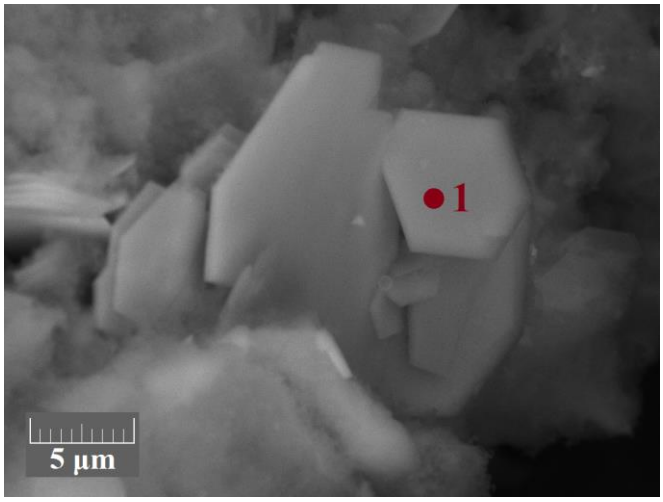

Figure 8. SEM image of an area in the solid residue obtained by leaching of the WAT sample using 10% HCl at 150 °C and S:L ratio = 1:11 for 60 min.

Table 2. Elemental composition (at. %) of the sample point signed in Figure 8.

Sign	Al	Si	Ti	Ca	Mg	Cl	O
1	21.6	5.2	2.3	1.6	1.4	0.2	67.6

Table 3 shows that the residues obtained by HPAL using the diluted and the concentrated acids contain different amounts of SiO_2 and TiO_2, as well as a similar amount of Al_2O_3. The residue obtained by HPAL using 20% HCl at 210 °C has a lower Al_2O_3 and MgO amount compared with the residues obtained at lower temperatures and acid con-

Preprints (www.preprints.org) | NOT PEER-REVIEWED | Posted: 1 February 2021 doi:10.20944/preprints202102.0065.v1

centration. These data substantiate the above-mentioned leaching mechanism for the WAT leaching.

Table 3. Chemical composition of the solid residues obtained by the leaching of the WAT sample at S:L ratio = 1:11 for 60 min (wt. %).

HPAL conditions	Al_2O_3	CaO	MgO	SiO_2	TiO_2	S
10% HCl, 190 °C	9.36	1.30	1.38	59.1	22.5	0.15
20% HCl, 150 °C	8.47	1.43	1.74	71.6	9.64	0.24
20% HCl, 210 °C	1.29	0.32	1.02	77.0	14.6	0.25

Figure 3 demonstrates that REE dissolution is sharply increased at temperatures for both acid concentrations above 110 °C and 90 °C, respectively, that is likely due to the dissolution of $CaTiO_3$ (Figure 7). REEs can be associated with perovskite in a form of solid solution [59]. It was reported that Sc in the slag obtained after red mud reduction smelting is associated with $CaTiO_3$ [29] and with Ti in the initial red mud [60]. It should be mentioned that Sc also can be partially associated with grossular [53].

In summary, it can be inferred that the leaching temperature of 150 °C and acid concentration of 10% are the optimal conditions for the WAT treatment that led to passing into solution of 91% Sc and above 80% of other REEs and remaining of TiO_2 and SiO_2 in the residue. It should be noted that small aluminum losses with the residue are inevitable.

3.2.2. The solid residues obtained from the SSAT sample

Figure 9 shows the results of the SEM-EDX analysis of the residue obtained by HPAL of the SSAT sample using 10% HCl at 170 °C. One can see from the images that the SSAT residue, like the WAT sample, mainly consists of amorphous SiO_2 and titanium oxide. Moreover, sulfur can be observed in the form of particular grains. It is noteworthy that the distribution of aluminum and magnesium correlates that clearly points out to the presence of $MgAl_2O_4$.

The generation of elemental sulfur during HPAL is probably due to the following mechanism. It is clear that calcium sulfide containing in the tailings interacts with hydrochloric acid forming hydrogen sulfide:

$$CaS_{(s)} + 2HCl_{(l)} = CaCl_{2(l)} + H_2S_{(g)}, \quad (7)$$

Then hydrogen sulfide can react with atmospheric oxygen in gaseous phase with precipitation of sulfur [61]:

$$2H_2S_{(g)} + O_{2(g)} = 2S_{(s)}\downarrow + 2H_2O_{(g)}, \quad (8)$$

$$2H_2S_{(g)} + O_{2(g)} = 2SO_{2(g)} + 2H_2O_{(g)}, \quad (9)$$

$$2H_2S_{(g)} + SO_{2(g)} = 3S\downarrow + 2H_2O_{(g)}. \quad (10)$$

Moreover, sulfur forms quite likely by interaction of hydrogen sulfide and ferric chloride [62]:

$$CaS_{(s)} + 2HCl_{(l)} = CaCl_{2(l)} + H_2S_{(g)}, \quad (11)$$

Preprints (www.preprints.org) | NOT PEER-REVIEWED | Posted: 1 February 2021 doi:10.20944/preprints202102.0065.v1

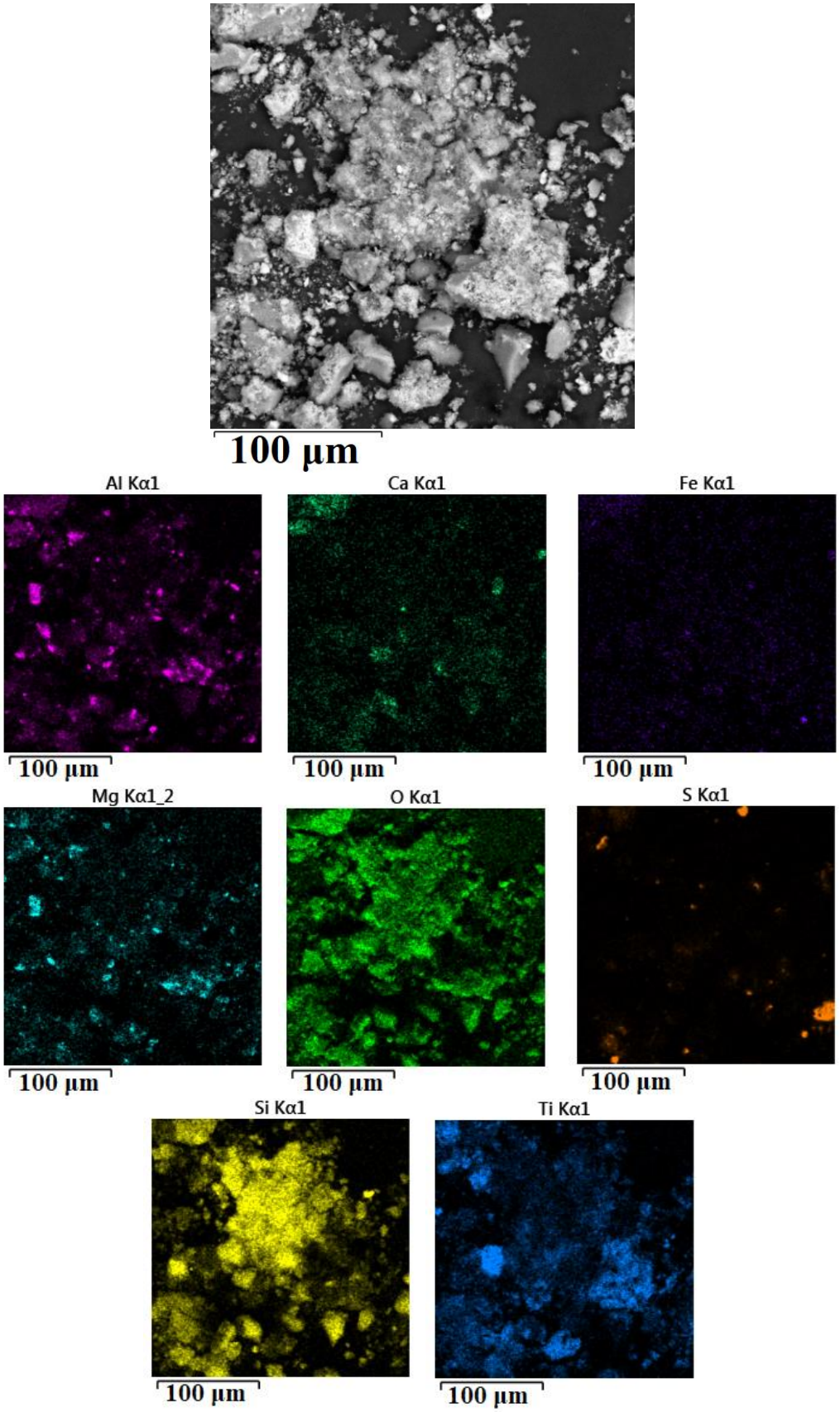

Figure 9. SEM images with the distribution of elements in the solid residue obtained by the leaching of the SSAT sample using 10% HCl at 170 °C and S:L ratio = 1:11 for 60 min.

Figure 10 shows the XRD patterns of the SSAT residues obtained at different leaching temperatures using both the HCl concentrations.

Preprints (www.preprints.org) | NOT PEER-REVIEWED | Posted: 1 February 2021 doi:10.20944/preprints202102.0065.v1

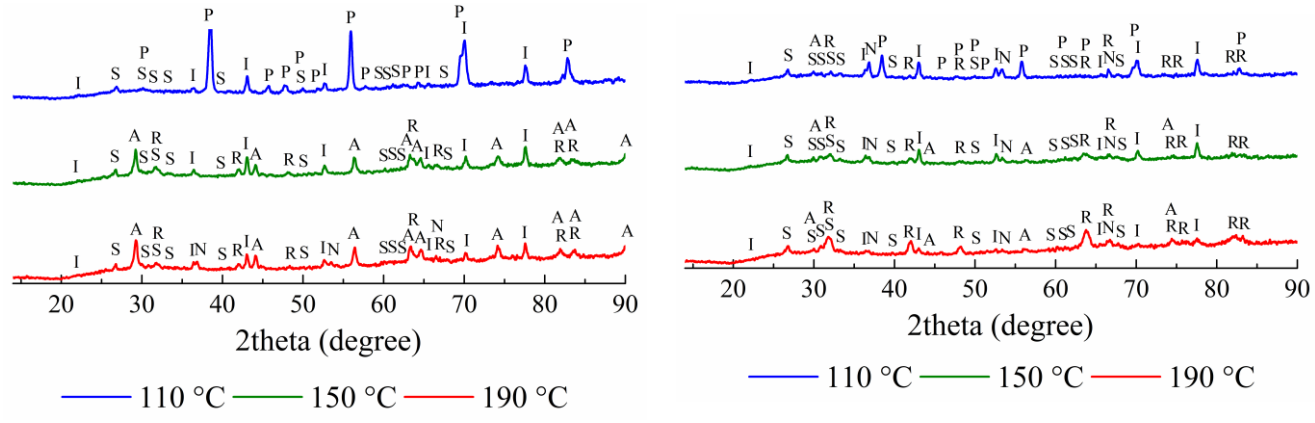

Figure 10. The XRD patterns of the solid residues after the leaching of SSAT sample using 10% (**a**) and 20% HCl (**b**), where P – $CaTiO_3$; A – TiO_2 (anatase); R – TiO_2 (rutile); S – sulfur (α-S_8); D – $5Al_2O_3 \cdot H_2O$; N – NaCl; I – $MgAl_2O_4$.

The SSAT sample contains only one aluminum-containing phase, namely, $NaAlSiO_4$, which is more soluble in acid solutions compared with $Ca_3Al_2Si_3O_{12}$ and $Ca_2Al_2SiO_7$ phases that is clearly seen from the XRD spectra. Nonetheless, aluminum passed into solution incompletely even at high temperatures and acid concentrations due to the formation of $5Al_2O_3 \cdot H_2O$ and $MgAl_2O_4$ phases. Table 4 gives the elemental composition of the residues obtained by HPAL of the SSAT sample using the diluted and the concentrated acids. They mainly contain SiO_2 and TiO_2 that indicated to the same dissolution behavior of Ti and Si during leaching of the SSAT and WAT samples alike.

Table 4. Chemical composition of the solid residues obtained by the leaching of the SSAT sample at S:L ratio = 1:11 for 60 min (wt. %).

HPAL conditions	Al_2O_3	CaO	MgO	SiO_2	TiO_2	S
10% HCl, 90 °C	9.18	10.7	2.17	38.8	14.4	7.22
10% HCl, 210 °C	7.09	1.68	1.30	50.4	20.0	4.02
20% HCl, 130 °C	11.3	3.22	2.51	46.3	5.68	8.5
20% HCl, 210 °C	2.94	1.23	0.38	52.8	16.5	8.7

As can be seen from Figures 3 and 5, the extraction degrees of Sc for the SSAT sample were lower compared to the WAT sample that is probably owing to an increase of pH solution due to dissolution of sodium. It is well-known that an increase of pH value of the solution led to a decrease of Sc extraction [45,46]. It is previously reported [53] that a significant part of Y and Sc can be associated with $NaAlSiO_4$ in the tailings obtained after carbothermic roasting of red mud with the addition of sodium salts, but the present investigation has shown that there were no positive correlation between their dissolution. On the contrary, SEM-EDX analysis of the residue obtained by HPAL of the SSAT sample (Figure 11 and Table 4) indicates clearly that Sc along with Zr are predominantly associated with titanium. The detected presence of zirconium and scandium together and an increase of the Sc extraction degree with Zr dissolution degree rise in 20% HCl (Figures 3 and 5) enable to assume that a minor part of scandium is probably associated with zirconium minerals that is consistent with the results of authors [62], which noted that 10% of the total Sc is associated with $ZrSiO_4$ in red mud.

Preprints (www.preprints.org) | NOT PEER-REVIEWED | Posted: 1 February 2021 doi:10.20944/preprints202102.0065.v1

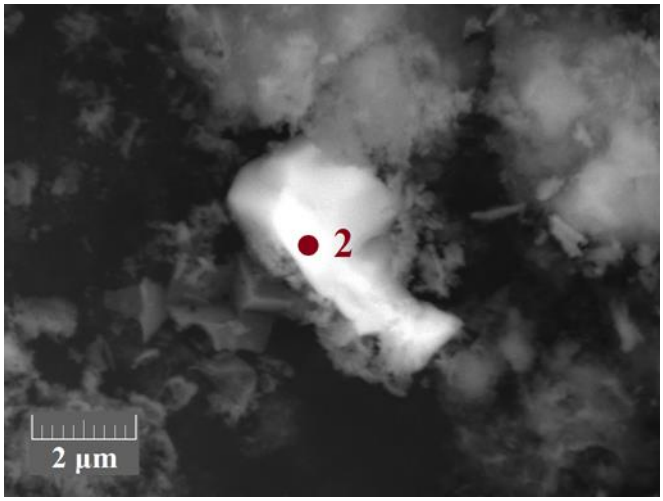

Figure 11. SEM image of an area in the solid residue obtained by the leaching of the SSAT sample using 10% HCl at 170 °C and S:L ratio = 1:11 for 60 min.

Table 4. Elemental composition (at. %) of the sample point signed in Figure 11.

Sign	Al	Si	Ti	Ca	Mg	Zr	Sc	S	Cl	O
2	2.6	5.2	20.7	5.4	0.8	3.2	1.4	0.6	0.3	59.7

The optimal leaching conditions for the SSAT sample, which allows to extract 91% Al, 75% Sc, 63% Y, and more than 78% of other REEs, are 150 °C and 20% HCl concentration. However, it should be appreciated that about 26% Ti also passed into the solution under these conditions.

3.3. HPAL experiments with variation of leaching time, S:L ratio, and HCl concentration

The performed experiments have pointed out that using of HPAL with hydrochloric acid for the WAT sample is more preferable compared to the SSAT sample due to enabling of selective separation of titanium and silicon from the other elements. To elucidate a dissolution behavior of the most important elements in the WAT sample, a set of the experiments at the optimal temperature with a variation of different leaching parameters was carried out. Figure 12 illustrates the influence of leaching duration on recovery degree of aluminum, titanium, iron, and scandium. An increase of leaching time led to insignificant growth of the extraction degree of Sc and Al for both the acid concentrations. Moreover, the decrease of leaching time led to an increase of Ti extraction degree that negatively effects on the process selectivity.

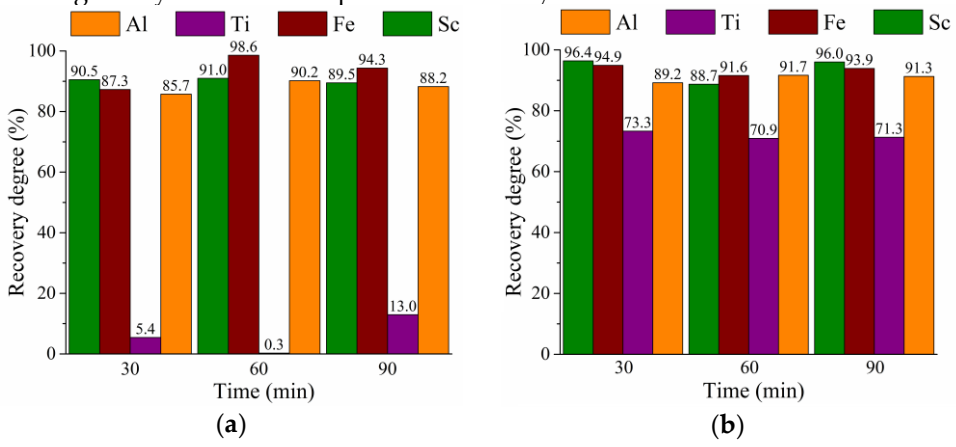

Figure 12. Effect of leaching time on the recovery degree of Al, Ti, Fe, Sc at 150 °C and S:L = 1:11 using 10% (**a**) and 20% (**b**) HCl.

Preprints (www.preprints.org) | NOT PEER-REVIEWED | Posted: 1 February 2021 doi:10.20944/preprints202102.0065.v1

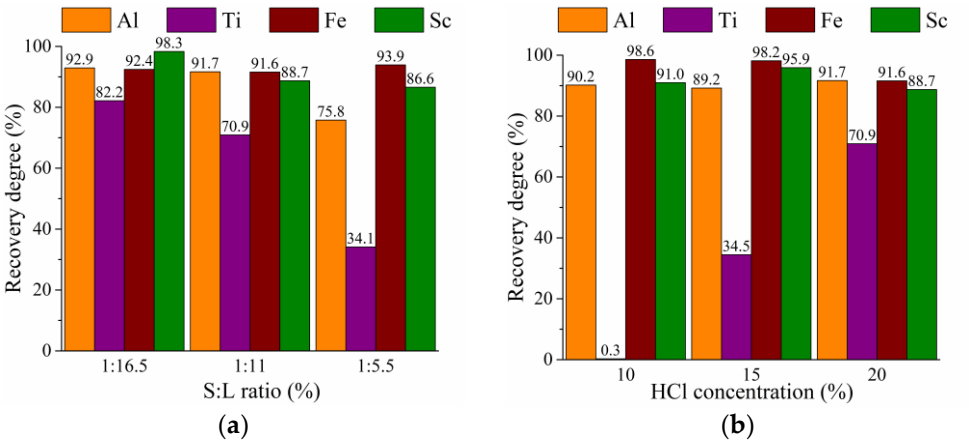

Figure 13. Effect of S:L ratio on the recovery degree of Al, Ti, Fe, Sc at 150 °C and 20% HCl (**a**) and effect of HCl concentration on recovery degree of Al, Ti, Fe, Sc at 150 °C and S:L = 1:11 (**b**).

Figure 13 demonstrates the influence of S:L ratio and concentration of the acid on the recovery degree of aluminum, titanium, iron, and scandium. As can be seen, the dissolution degree of Ti drastically grows up with an increase of acid concentration and S:L ratio that is consistent with equation (6). It has to be taken into account that an increase of S:L ratio led to a drop not only aluminum extraction degree, but also scandium extraction degree that accords with previous studies [63,64].

4. Discussion

The HPAL of the tailings using the diluted hydrochloric acid allows to separate selectively REEs and Al from Ti and SiO_2 with high effectivity. The obtained residue can contain more than 20% TiO_2 and over 50% SiO_2 (Table 3) that indicates it as a valuable raw material for Ti extraction. To extract Ti, various leaching treatment was suggested using the mixture of hydrogen peroxide and sulfuric acid with suppression of Si dissolution [65], as well as using alkaline solutions [66], phosphoric acid [45], etc. However, the most promising way for Ti extraction from the residue is the leaching by concentrated hydrochloric acid with its dissolution and subsequent precipitation of TiO_2 [67]. The obtained amorphous SiO_2 can be used for production of white carbon black [68].

REEs can be relatively simply recovered from the leached solutions by well-known methods, e.g., solvent extraction, ion-exchange sorption, selective precipitation, etc. [69]. The remaining aluminum chloride solution can be used as a coagulant for water treatment [57,70] or as a raw material for the production of metallurgical alumina [71]. Thus, a two-step hydrochloric acid leaching process can be implemented.

As reflected by Figure 13, the application of 20% HCl with S:L ratio of 1:16.5 led to a considerable rise of Al, Ti, Sc extraction degree that enables to consider simultaneous dissolution of these elements with a following stepwise extraction of REEs and titanium from the leached solution. Moreover, after the REE extraction, Al-Ti-containing solution can be regarded as a complex coagulant, which has an increased efficiency for waste water treatment compared with the Ti-free solutions [72,73]. However, it should be noted that the use of excess of acid and liquid-to-solid ratio during HPAL deteriorates cost efficiency of the process, so a feasibility study is necessary.

The application of HPAL method using HCl led to a similar Al recovery for the WAT and SSAT samples, but the treatment of the SSAT resulted in a rather lower Sc recovery and a slightly higher acid consumption. Furthermore, the residue obtained by the leaching of the SSAT sample can contain a substantial percentage of elemental sulfur and sodium chloride, so additional stages for their removal is necessary. To remove NaCl, washing by water can be applied, and to extract elemental sulfur, distillation [74] or flotation [75] can be used. Despite the mentioned disadvantages of the SSAT leaching, total cost of red mud processing using sodium sulfate may be lower owing to reduced

Preprints (www.preprints.org) | NOT PEER-REVIEWED | Posted: 1 February 2021 doi:10.20944/preprints202102.0065.v1

roasting temperature and improved grindability of the roasted sample. In any case, a comparative economic assessment of the treatment of the WAT and SSAT samples is required.

Figure 14 shows two principal flowsheets of red mud processing developed as a result of the study.

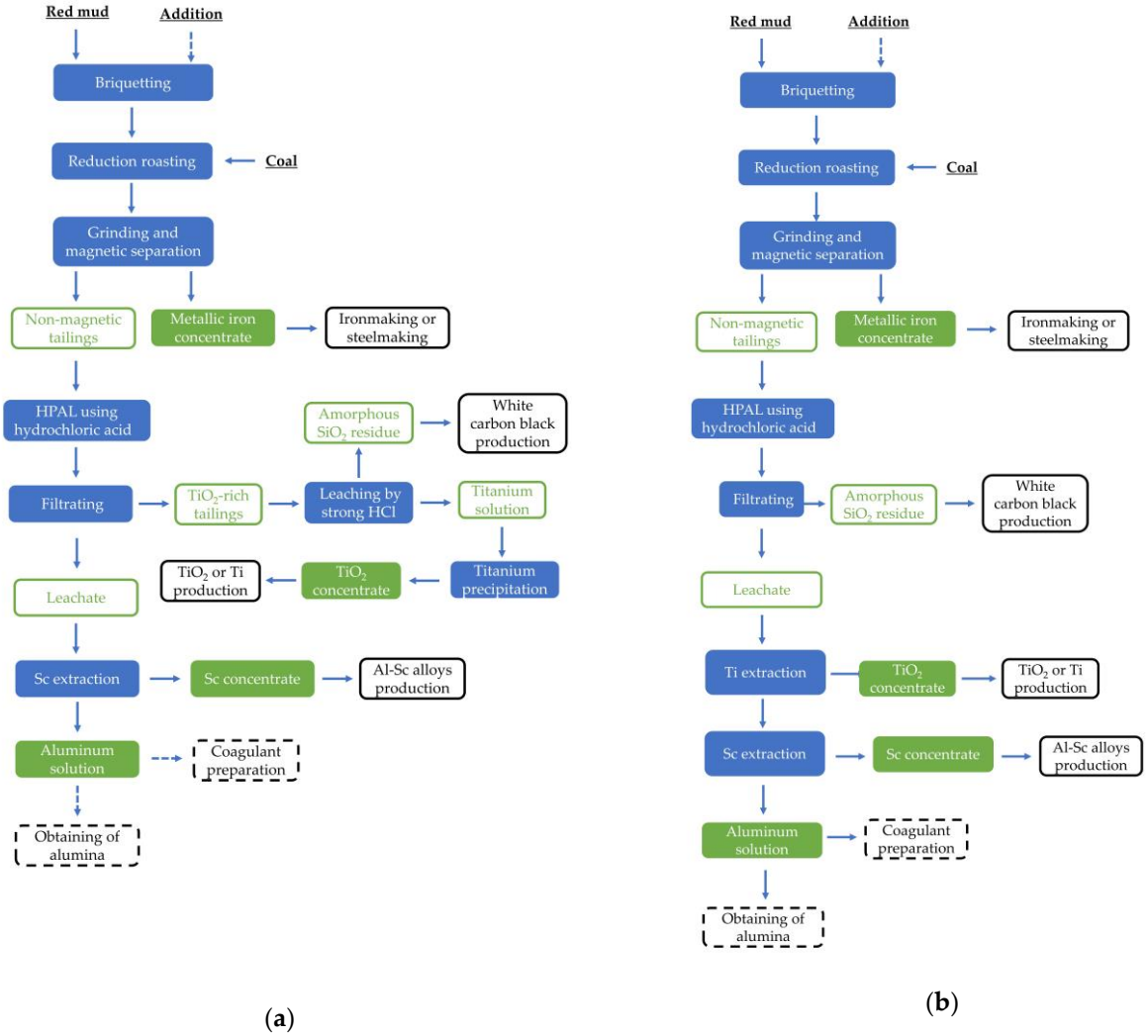

Figure 14. The flowsheets of red mud processing using two (**a**) and one (**b**) leaching stages.

5. Conclusions

The application of HPAL using hydrochloric acid for the extraction of Al and REEs from non-magnetic residues obtained from red mud after iron removal has shown a high effectivity. The leaching of valuable elements from the WAT sample is probably more preferable than from the SSAT sample.

For the WAT sample, the optimal leaching conditions, which are leaching temperature of 150 °C, acid concentration of 10%, solid-to-liquid ratio of 1:11, and duration of 60 min, led to passing into solution of 90% Al, 91% Sc and above 80% of other REEs, as well as remaining of TiO_2 and SiO_2 in the residue. To dissolve titanium along with Al and REEs, the temperature of 150 °C, acid concentration of 20%, solid-to-liquid ratio of 1:16.5, and duration of 60 min can be applied that allowed to extract 93% Al, 82% Ti, 98% Sc.

For the SSAT sample, 91% Al, 75% Sc, above 60% of other REEs, and 26% Ti were dissolved under the optimal conditions, which were leaching temperature of 150 °C, acid concentration of 20%, solid-to-liquid ratio of 1:11, and duration of 60 min.

Based on HPAL using hydrochloric acid, two flowsheets were proposed for the treatment of both kinds of non-magnetic tailings.

Author Contributions: Conceptualization, D.Z. and P.G.; Methodology, D.Z., P.G., and A.V.; Investigation, E.Z., D.G., and A.V.; Resources, V.D.; Writing — original draft preparation, D.Z. and P.G.; Writing — review and editing, A.V..; Visualization, P.G. and D.G.; Supervision, V.D. and A.P.; Project administration, V.D. and A.P.; Funding acquisition, A.P. All authors have read and agreed to the published version of the manuscript.

Funding: The present study was funded by RFBR according to Research Project No. 18–29–24186. Access to the electronic database of scientific publications was provided within Russian state assignment No. 075-00328-21-00.

Acknowledgments: The authors would like to appreciate The Center for Collective Use Testing Analytical Center of the JSC "Scientific-research institute of chemical technology" for chemical analysis and to express profound appreciation to Dr. Dmitry Valeev for valuable remarks and discussion of the manuscript.

Conflicts of Interest: The authors declare no conflict of interest.

References

1. Zeng, H.; Lyu, F.; Sun, W.; Zhang, H.; Wang, L.; Wang, Y. Progress on the industrial applications of red mud with a focus on China. *Minerals* **2020**, *10*, 773. DOI: 10.3390/min10090773.
2. Wang, L.; Sun, N.; Tang, H.; Sun, W. A Review on Comprehensive Utilization of Red Mud. *Minerals* **2019**, *9*, 362. DOI: 10.3390/min9060362.
3. Service, R.F. Red mud is piling up. Can scientists figure out what to do with it? Available online: https://www.sciencemag.org/news/2020/08/red-mud-piling-can-scientists-figure-out-what-do-it (accessed on Nov 25, 2020).
4. Archambo, M.; Kawatra, S.K. Red Mud: Fundamentals and New Avenues for Utilization. *Miner. Process. Extr. Metall. Rev.* **2020**, 1–24. DOI: 10.1080/08827508.2020.1781109.
5. Wang, S.; Ang, H.M.; Tadé, M.O. Novel applications of red mud as coagulant, adsorbent and catalyst for environmentally benign processes. *Chemosphere* **2008**, *72*, 1621–1635. DOI: 10.1016/j.chemosphere.2008.05.013.
6. Joseph, C.G.; Taufiq-Yap, Y.H.; Krishnan, V.; Li Puma, G. Application of modified red mud in environmentally-benign applications: A review paper. *Environ. Eng. Res.* **2020**, *25*, 795–806. DOI: 10.4491/eer.2019.374.
7. Khairul, M.A.; Zanganeh, J.; Moghtaderi, B. The composition, recycling and utilisation of Bayer red mud. *Resour. Conserv. Recycl.* **2019**, *141*, 483–498. DOI: 10.1016/j.resconrec.2018.11.006.
8. Liu, Y.; Naidu, R. Hidden values in bauxite residue (red mud): Recovery of metals. *Waste Manag.* **2014**, *34*, 2662–2673. DOI: 10.1016/j.wasman.2014.09.003.
9. Akcil, A.; Akhmadiyeva, N.; Abdulvaliyev, R.; Meshram, A.; Meshram, P. Overview On Extraction and Separation of Rare Earth Elements from Red Mud: Focus on Scandium. *Miner. Process. Extr. Metall. Rev.* **2018**, *39*, 145–151. DOI: 10.1080/08827508.2017.1288116.
10. Kumar, S.; Kumar, R.; Bandopadhyay, A. Innovative methodologies for the utilisation of wastes from metallurgical and allied industries. *Resour. Conserv. Recycl.* **2006**, *48*, 301–314. DOI: 10.1016/j.resconrec.2006.03.003.
11. Tuck, C.A. Iron Ore Data Sheet Available online: https://pubs.usgs.gov/periodicals/mcs2020/mcs2020-iron-ore.pdf (accessed on Nov 24, 2020).
12. Liu, Z.; Li, H. Metallurgical process for valuable elements recovery from red mud - A review. *Hydrometallurgy* **2015**, *155*, 29–43. DOI: 10.1016/j.hydromet.2015.03.018.
13. Avdibegović, D.; Regadío, M.; Binnemans, K. Efficient separation of rare earths recovered by a supported ionic liquid from bauxite residue leachate. *RSC Adv.* **2018**, *8*, 11886–11893. DOI: 10.1039/c7ra13402a.

14. Meng, F.; Li, X.; Wang, P.; Yang, F.; Liang, D.; Gao, F.; He, C.; Wei, Y. Recovery of Scandium from Bauxite Residue by Selective Sulfation Roasting with Concentrated Sulfuric Acid and Leaching. *JOM* **2020**, *72*, 816–822. DOI: 10.1007/s11837-019-03931-9.
15. Narayanan, R.P.; Kazantzis, N.K.; Emmert, M.H. Selective Process Steps for the Recovery of Scandium from Jamaican Bauxite Residue (Red Mud). *ACS Sustain. Chem. Eng.* **2018**, *6*, 1478–1488. DOI: 10.1021/acssuschemeng.7b03968.
16. Bayca, S.U.; Kisik, H. Optimization of leaching parameters of aluminum hydroxide extraction from bauxite waste using the taguchi method. *Environ. Prog. Sustain. Energy* **2018**, *37*, 196–202. DOI: 10.1002/ep.12654.
17. Vaylert, A. V.; Pyagay, I.N.; Kozhevnikov, V.L.; Pasechnik, L.A.; Yatsenko, S.P. Autoclave hydrometallurgical processing of alumina production red mud. *Tsvetnye Met.* **2014**, *3*, 27–31.
18. Shoppert, A.A.; Loginova, I.V. Red Mud as an Additional Source of Titanium Raw Materials. *KnE Mater. Sci.* **2017**, *2*, 150–157. DOI: 10.18502/kms.v2i2.962.
19. Agrawal, S.; Dhawan, N. Investigation of mechanical and thermal activation on metal extraction from red mud. *Sustain. Mater. Technol.* **2021**, *27*, e00246. DOI: 10.1016/j.susmat.2021.e00246.
20. Reid, S.; Tam, J.; Yang, M.; Azimi, G. Technospheric Mining of Rare Earth Elements from Bauxite Residue (Red Mud): Process Optimization, Kinetic Investigation, and Microwave Pretreatment. *Sci. Rep.* **2017**, *7*, 1–9. DOI: 10.1038/s41598-017-15457-8.
21. Ochsenkuehn-Petropoulou, M.; Tsakanika, L.-A.; Lymperopoulou, T.; Ochsenkuehn, K.-M.; Hatzilyberis, K.; Georgiou, P.; Stergiopoulos, C.; Serifi, O.; Tsopelas, F. Efficiency of Sulfuric Acid on Selective Scandium Leachability from Bauxite Residue. *Metals (Basel).* **2018**, *8*, 915. DOI: 10.3390/met8110915.
22. Xie, W.; Zhang, N.; Li, J.; Zhou, F.; Ma, X.; Gu, G.; Zhang, W. Optimization of condition for extraction of aluminum and iron from red mud by hydrochloric acid leaching. *Chinese J. Environ. Eng.* **2017**, *11*, 5677–5682. DOI: 10.12030/j.cjee.201611059.
23. Alkan, G.; Schier, C.; Gronen, L.; Stopic, S.; Friedrich, B. A Mineralogical Assessment on Residues after Acidic Leaching of Bauxite Residue (Red Mud) for Titanium Recovery. *Metals (Basel).* **2017**, *7*, 458. DOI: 10.3390/met7110458.
24. Zhu, X.; Niu, Z.; Li, W.; Zhao, H.; Tang, Q. A novel process for recovery of aluminum, iron, vanadium, scandium, titanium and silicon from red mud. *J. Environ. Chem. Eng.* **2019**, *8*, 103528. DOI: 10.1016/j.jece.2019.103528.
25. Gu, H.; Li, W.; Li, Z.; Guo, T.; Wen, H.; Wang, N. Leaching Behavior of Lithium from Bauxite Residue Using Acetic Acid. *Mining, Metall. Explor.* **2020**, *37*, 443–451. DOI: 10.1007/s42461-020-00181-1.
26. Atalay Kalsen, T.S.; Karadağ, H.B.; Eker, Y.R.; Kerti, I. Chemical Composition Simplification of the Seydişehir (Konya, Turkey) Alumina Plant Waste. *J. Sustain. Metall.* **2019**, *5*, 482–496. DOI: 10.1007/s40831-019-00236-8.
27. Davris, P.; Balomenos, E.; Panias, D.; Paspaliaris, I. Selective leaching of rare earth elements from bauxite residue (red mud), using a functionalized hydrophobic ionic liquid. *Hydrometallurgy* **2016**, *164*, 125–135. DOI: 10.1016/j.hydromet.2016.06.012.
28. Onghena, B.; Binnemans, K. Recovery of Scandium(III) from aqueous solutions by solvent extraction with the functionalized ionic liquid betainium bis(trifluoromethylsulfonyl)imide. *Ind. Eng. Chem. Res.* **2015**, *54*, 1887–1898. DOI: 10.1021/ie504765v.
29. Rivera, R.M.; Xakalashe, B.; Ounoughene, G.; Binnemans, K.; Friedrich, B.; Van Gerven, T. Selective rare earth element extraction using high-pressure acid leaching of slags arising from the smelting of bauxite residue. *Hydrometallurgy* **2019**, *184*, 162–174. DOI: 10.1016/j.hydromet.2019.01.005.
30. Zinoveev, D.V.; Grudinskii, P.I.; Dyubanov, V.G.; Kovalenko, L.V.; Leont'ev, L.I. Global recycling experience of red mud – A review. Part I: Pyrometallurgical methods. *Izv. Ferr. Metall.* **2018**, *61*, 843–858. DOI: 10.17073/0368-0797-2018-11-843-858.
31. Alkan, G.; Xakalashe, B.; Yagmurlu, B.; Kaußen, F.; Friedrich, B. Conditioning of red mud for subsequent titanium and scandium recovery - A conceptual design study. *World Metall. - ERZMETALL* **2017**, *70*, 5–12.
32. Balomnenos, E.; Kastritis, D.; Panias, D.; Paspaliaris, I.; Boufounos, D. The Enexal Bauxite Residue Treatment Process: Industrial Scale Pilot Plant Results. In *Light Metals 2014*; Grandfield, J., Ed.; Springer: Cham, Switzerland, 2014; pp. 143–147. DOI: 10.1007/978-3-319-48144-9_25.

33. Ning, G.; Zhang, B.; Liu, C.; Li, S.; Ye, Y.; Jiang, M. Large-Scale Consumption and Zero-Waste Recycling Method of Red Mud in Steel Making Process. *Minerals* **2018**, *8*, 102. DOI: 10.3390/min8030102.
34. Borra, C.R.; Blanpain, B.; Pontikes, Y.; Binnemans, K.; Van Gerven, T. Recovery of Rare Earths and Major Metals from Bauxite Residue (Red Mud) by Alkali Roasting, Smelting, and Leaching. *J. Sustain. Metall.* **2017**, *3*, 393–404. DOI: 10.1007/s40831-016-0103-3.
35. Chun, T.J.; Zhu, D.Q.; Pan, J.; He, Z. Preparation of metallic iron powder from red mud by sodium salt roasting and magnetic separation. *Can. Metall. Q.* **2014**, *53*, 183–189. DOI: 10.1179/1879139513y.0000000114.
36. Onghena, B.; Borra, C.R.; Van Gerven, T.; Binnemans, K. Recovery of scandium from sulfation-roasted leachates of bauxite residue by solvent extraction with the ionic liquid betainium bis(trifluoromethylsulfonyl)imide. *Sep. Purif. Technol.* **2017**, *176*, 208–219. DOI: 10.1016/j.seppur.2016.12.009.
37. Zinoveev, D.; Grudinsky, P.; Zakunov, A.; Semenov, A.; Panova, M.; Valeev, D.; Kondratiev, A.; Dyubanov, V.; Petelin, A. Influence of Na_2CO_3 and K_2CO_3 addition on iron grain growth during carbothermic reduction of red mud. *Metals (Basel).* **2019**, *9*, 1313. DOI: 10.3390/met9121313.
38. Chun, T.; Li, D.; Di, Z.; Long, H.; Tang, L.; Li, F.; Li, Y. Recovery of iron from red mud by hightemperature reduction of carbonbearing briquettes. *J. South. African Inst. Min. Metall.* **2017**, *117*, 361–364. DOI: 10.17159/2411-9717/2017/v117n4a7.
39. Zhang, B.; Liu, C.; Li, C.; Jiang, M. A novel approach for recovery of rare earths and niobium from Bayan Obo tailings. *Miner. Eng.* **2014**, *65*, 17–23. DOI: 10.1016/j.mineng.2014.04.011.
40. Ding, W.; Peng, Y.; Wu, Q.; Shen, S.; Xiao, J.; Liang, G.; Huang, W. Increase of iron concentration and reduction of impurities in red mud from the Wenshan area of Yunnan Province by segregation roasting-low intensity magnetic separation. *J. Mines, Met. Fuels* **2019**, *67*, 377–384.
41. Gao, F.; Zhang, J.; Deng, X.; Wang, K.; He, C.; Li, X.; Wei, Y. Comprehensive Recovery of Iron and Aluminum from Ordinary Bayer Red Mud by Reductive Sintering–Magnetic Separation–Digesting Process. *JOM* **2019**, *71*, 2936–2943. DOI: 10.1007/s11837-018-3311-4.
42. Li, G.; Luo, J.; Jiang, T.; Li, Z.; Peng, Z.; Zhang, Y. Digestion of alumina from non-magnetic material obtained from magnetic separation of reduced iron-rich diasporic bauxite with sodium salts. *Metals (Basel).* **2016**, *6*, 294. DOI: 10.3390/met6110294.
43. Li, G.; Liu, M.; Rao, M.; Jiang, T.; Zhuang, J.; Zhang, Y. Stepwise extraction of valuable components from red mud based on reductive roasting with sodium salts. *J. Hazard. Mater.* **2014**, *280*, 774–780. DOI: 10.1016/j.jhazmat.2014.09.005.
44. Rivera, R.M.; Ulenaers, B.; Ounoughene, G.; Binnemans, K. Behaviour of Silica during Metal Recovery from Bauxite Residue by Acidic Leaching. In Proceedings of the 35th International ICSOBA Conference, Hamburg, Germany, 2 – 5 October, 2017; Hamburg, Germany, 2017; pp. 547–556.
45. Deng, B.; Li, G.; Luo, J.; Ye, Q.; Liu, M.; Peng, Z.; Jiang, T. Enrichment of Sc_2O_3 and TiO_2 from bauxite ore residues. *J. Hazard. Mater.* **2017**, *331*, 71–80. DOI: 10.1016/j.jhazmat.2017.02.022.
46. Borra, C.R.; Blanpain, B.; Pontikes, Y.; Binnemans, K.; Van Gerven, T. Smelting of Bauxite Residue (Red Mud) in View of Iron and Selective Rare Earths Recovery. *J. Sustain. Metall.* **2016**, *2*, 28–37. DOI: 10.1007/s40831-015-0026-4.
47. Valeev, D.; Kunilova, I.; Alpatov, A.; Mikhailova, A.; Goldberg, M.; Kondratiev, A. Complex utilisation of ekibastuz brown coal fly ash: Iron & carbon separation and aluminum extraction. *J. Clean. Prod.* **2019**, *218*, 192–201. DOI: https://doi.org/10.1016/j.jclepro.2019.01.342.
48. Li, S.; Qin, S.; Kang, L.; Liu, J.; Wang, J.; Li, Y. An Efficient Approach for Lithium and Aluminum Recovery from Coal Fly Ash by Pre-Desilication and Intensified Acid Leaching Processes. *Metals (Basel).* **2017**, *7*, 272. DOI: 10.3390/met7070272.
49. Grudinsky, P.; Zinoveev, D.; Pankratov, D.; Semenov, A.; Panova, M.; Kondratiev, A.; Zakunov, A.; Dyubanov, V.; Petelin, A. Influence of Sodium Sulfate Addition on Iron Grain Growth during Carbothermic Roasting of Red Mud Samples with Different Basicity. *Metals (Basel).* **2020**, *10*, 1571. DOI: 10.3390/met10121571.
50. *Match!*, version 3.11; software for identification of powder diffraction patterns; Crystal Impact: Bonn, Germany, 2021.

51. Han, J.; Zhang, J.; Feng, W.; Chen, X.; Zhang, L.; Tu, G. A clean process to prepare high-quality acid-soluble titanium slag from titanium middling ore. *Minerals* **2019**, *9*, 460. DOI: 10.3390/min9080460.
52. Liu, Y.; Shao, D.; Wang, W.; Yi, L.; Chen, D.; Zhao, H.; Wu, J.; Qi, T.; Cao, C. Preparation of rutile TiO_2 by hydrolysis of $TiOCl_2$ solution: Experiment and theory. *RSC Adv.* **2016**, *6*, 59541–59549. DOI: 10.1039/c6ra04386k.
53. Deng, B.; Li, G.; Luo, J.; Ye, Q.; Liu, M.; Rao, M.; Jiang, T.; Bauman, L.; Zhao, B. Selectively leaching the iron-removed bauxite residues with phosphoric acid for enrichment of rare earth elements. *Sep. Purif. Technol.* **2019**, *227*, 115714. DOI: 10.1016/j.seppur.2019.115714.
54. Wajima, T. Effects of step-wise acid leaching with HCl on synthesis of zeolitic materials from paper sludge ash. *Minerals* **2020**, *10*, 402. DOI: 10.3390/min10050402.
55. Rivera, R.M.; Ulenaers, B.; Ounoughene, G.; Binnemans, K.; Van Gerven, T. Extraction of rare earths from bauxite residue (red mud) by dry digestion followed by water leaching. *Miner. Eng.* **2018**, *119*, 82–92. DOI: 10.1016/j.mineng.2018.01.023.
56. Yu, W.; Wen, X.; Chen, J.; Tang, Q.; Dong, W.; Zhong, J. Effect of Sodium Borate on the Preparation of TiN from Titanomagnetite Concentrates by Carbothermic Reduction – Magnetic Separation and Acid Leaching Process. *Minerals* **2019**, *9*, 675. DOI: 10.3390/min9110675.
57. Zhao, Y.; Zheng, Y.; He, H.; Sun, Z.; Li, A. Effective aluminum extraction using pressure leaching of bauxite reaction residue from coagulant industry and leaching kinetics study. *J. Environ. Chem. Eng.* **2020** (in press). DOI: 10.1016/j.jece.2020.104770.
58. Digne, M.; Sautet, P.; Raybaud, P.; Toulhoat, H.; Artacho, E. Structure and stability of aluminum hydroxides: A theoretical study. *J. Phys. Chem. B* **2002**, *106*, 5155–5162. DOI: 10.1021/jp014182a.
59. Shrivastava, O.P.; Kumar, N.; Sharma, I.B. Solid state synthesis and structural refinement of polycrystalline $La_xCa_{1-x}TiO_3$ ceramic powder. *Bull. Mater. Sci.* **2004**, *27*, 121–126. DOI: 10.1007/BF02708493.
60. Anawati, J.; Azimi, G. Recovery of scandium from Canadian bauxite residue utilizing acid baking followed by water leaching. *Waste Manag.* **2019**, *95*, 549–559. DOI: 10.1016/j.wasman.2019.06.044.
61. Steijns, M.; Derks, F.; Verloop, A.; Mars, P. The mechanism of the catalytic oxidation of hydrogen sulfide. II. Kinetics and mechanism of hydrogen sulfide oxidation catalyzed by sulfur. *J. Catal.* **1976**, *42*, 87–95. DOI: 10.1016/0021-9517(76)90094-4.
62. Vind, J.; Malfliet, A.; Bonomi, C.; Paiste, P.; Sajó, I.E.; Blanpain, B.; Tkaczyk, A.H.; Vassiliadou, V.; Panias, D. Modes of occurrences of scandium in Greek bauxite and bauxite residue. *Miner. Eng.* **2018**, *123*, 35–48. DOI: 10.1016/j.mineng.2018.04.025.
63. Huang, F.; Liao, Y.; Zhou, J.; Wang, Y.; Li, H. Selective recovery of valuable metals from nickel converter slag at elevated temperature with sulfuric acid solution. *Sep. Purif. Technol.* **2015**, *156*, 572–581. DOI: 10.1016/j.seppur.2015.10.051.
64. Borra, C.R.; Pontikes, Y.; Binnemans, K.; Van Gerven, T. Leaching of rare earths from bauxite residue (red mud). *Miner. Eng.* **2015**, *76*, 20–27. DOI: 10.1016/j.mineng.2015.01.005.
65. Alkan, G.; Yagmurlu, B.; Cakmakoglu, S.; Hertel, T.; Kaya, Ş.; Gronen, L.; Stopic, S.; Friedrich, B. Novel Approach for Enhanced Scandium and Titanium Leaching Efficiency from Bauxite Residue with Suppressed Silica Gel Formation. *Sci. Rep.* **2018**, *8*, 5676. DOI: 10.1038/s41598-018-24077-9.
66. Zablotskaya, Y. V.; Sadykhov, G.B.; Gocharenko, T. V. Autoclave leaching kinetics of a leucoxene concentrate with alkaline solutions. *Russ. Metall.* **2015**, *2015*, 3–7. DOI: 10.1134/S0036029515010140.
67. Wang, Z.; Liu, S.; Cao, X.; Wu, S.; Liu, C.; Li, G.; Jiang, W.; Wang, H.; Wang, N.; Ding, W. Preparation and characterization of TiO_2 nanoparticles by two different precipitation methods. *Ceram. Int.* **2020**, *46*, 15333–15341. DOI: 10.1016/j.ceramint.2020.03.075.
68. Yuan, W.; Yao, Z.; Zhang, Q.; Li, J. Characterization of residue from leached cathode ray tube funnel glass: reutilization as white carbon black. *J. Mater. Cycles Waste Manag.* **2014**, *16*, 629–634. DOI: 10.1007/s10163-014-0291-5.
69. Borra, C.R.; Blanpain, B.; Pontikes, Y.; Binnemans, K.; Van Gerven, T. Recovery of Rare Earths and Other Valuable Metals From Bauxite Residue (Red Mud): A Review. *J. Sustain. Metall.* **2016**, *2*, 365–386. DOI: 10.1007/s40831-016-0068-2.

70. Valeev, D.; Kunilova, I.; Shoppert, A.; Salazar-Concha, C.; Kondratiev, A. High-pressure HCl leaching of coal ash to extract Al into a chloride solution with further use as a coagulant for water treatment. *J. Clean. Prod.* **2020**, *276*, 123206. DOI: 10.1016/j.jclepro.2020.123206.
71. Valeev, D.; Shoppert, A.; Mikhailova, A.; Kondratiev, A. Acid and Acid-Alkali Treatment Methods of Al-Chloride Solution Obtained by the Leaching of Coal Fly Ash to Produce Sandy Grade Alumina. *Metals (Basel).* **2020**, *10*, 585. DOI: 10.3390/met10050585.
72. Azopkov, S. V.; Kuzin, E.N.; Kruchinina, N.E. Study of the Efficiency of Combined Titanium Coagulants in the Treatment of Formation Waters. *Russ. J. Gen. Chem.* **2020**, *90*, 1811–1816. DOI: 10.1134/S1070363220090364.
73. Kuzin, E.N.; Kruchinina, N.E. Purification of circulating and waste water in metallurgical industry using complex coagulants. *CIS Iron Steel Rev.* **2019**, *18*, 72–75. DOI: 10.17580/cisisr.2019.02.15.
74. Li, H.; Wu, X.; Wang, M.; Wang, J.; Wu, S.; Yao, X.; Li, L. Separation of elemental sulfur from zinc concentrate direct leaching residue by vacuum distillation. *Sep. Purif. Technol.* **2014**, *138*, 41–46. DOI: 10.1016/j.seppur.2014.09.036.
75. Liu, G.; Jiang, K.; Zhang, B.; Dong, Z.; Zhang, F.; Wang, F.; Jiang, T.; Xu, B. Selective Flotation of Elemental Sulfur from Pressure Acid Leaching Residue of Zinc Sulfide. *Minerals* **2021**, *11*, 89. DOI: 10.3390/min11010089.